Sixth International Conference on Durability of Concrete Structures
18 - 20 July 2018
University of Leeds, Leeds, West Yorkshire, LS2 9JT, United Kingdom

Paper Number RAM01

Monitoring Historic Concrete and Associated Cementitious Repair- A Case Study of Boathouse 4, Portsmouth Historic Dockyard, UK

A.H. Alwaal and S. Barnett
School of Civil Engineering and Surveying, University of Portsmouth, Portsmouth, UK

R. Inkpen and L. Hastewell
Department of Geography, University of Portsmouth, Portsmouth, UK

ABSTRACT

This study presents a method of monitoring historic concrete and associated repairs. A case study of Boathouse 4, Portsmouth Historic Dockyard, UK is presented. Boathouse 4 is an iconic building within Portsmouth Historic Dockyard which was constructed during the 1930's rearmament period. It was used during World War II to construct the three-man midget X-Craft submarine. The building was restored and converted into a Boatbuilding Skills Training Centre in 2015. A field investigation was conducted to analyse the concrete damage and to monitor microscale changes to the surface of the original concrete and repairs over a period of three years. Three patches of concrete lying in the undercroft of the building, located in an intertidal zone were chosen to be monitored for material changes as part of an ongoing PhD research study. These areas were scanned three times at intervals of up to 9 months within three years using a NextEngine portable laser scanner to obtain high-resolution 3D images of the concrete surface so that gradual changes to the microtopography, appearance and texture of the concrete surface and associated repairs could be detected. The data was analysed and the results indicated slight topographic changes in the concrete surface as well as the colour of the cementitious repair materials.

Keywords: historic concrete, topography, laser scanner, monitoring, repair materials

1.0 INTRODUCTION

Laser scanning is a non-destructive technique and it has been effectively employed in many fields such as architecture, civil engineering, geology, surveying and documentation of heritage sites. It can provide surface geometrical information in the form a three-dimensional model. Conservation and restoration of historic structures are among its main applications (Meroño *et al*., 2014).

The laser scanner measures the time taken by the pulse to go back to the instrument after the projection. It produces point clouds, each point has a particular coordinate in x, y and z plane.

Many studies have investigated the use of TLS in change detection, displacement and deformation monitoring of structures. The technique has been increasingly implemented to detect surface feature changes of rocks and stones (Swantesson *et al*., Brouste *et al.*) cited in (Schaefer and Inkpen, 2010).

Pagounis *et al*., (2016) examined geometric changes on a weathered ancient theatre made of soft-porous stones using terrestrial laser scanning and geodetic techniques. Another study was conducted by Moses (2014) on measuring rock surface weathering and erosion rate as well as surface roughness.

The technique has also been used in imaging concrete surfaces. A feasibility study using terrestrial laser scanner (TLS) showed promising results in using TLS as a detection technique on fire-damaged concrete structures. (Mukupa *et al*., 2016)

However, there are relatively few studies on the use of the laser scanning techniques on a concrete surface. Considering the ability of the technique to detect small-scale changes, its application in the growing field of monitoring and conserving heritage concrete buildings is being considered through PhD research by the first author. In this paper, relatively short-term changes on a concrete surface were assessed by considering standard deviation as a measure of surface variation and an indication of surface roughness.

2.0 THE STRUCTURE

Boathouse 4 (BH4) is a vast building located within Portsmouth Historic Dockyard, UK. The building (shown in Fig. 1) was constructed in the 1930s during the rearmament period prior the start of the World War II to construct the three-man midget X-Craft submarine.

Fig.1. External side and rear views of Boathouse 4 structure

2.1 The Undercroft

The iconic building is supported by concrete beams and columns located within the tidal zone. The tide typically rises to a midway level up the diagonal truss element (Fig. 2 (a)). The downstand beam and the slab soffit are normally above the tidal level. The undercroft can be accessed via a manhole in the floor slab of the building.

According to a condition assessment survey report conducted by Concrete Repairs Limited (CRL), deterioration and distress were found on the concrete elements forming the building mainly as a result of either chloride-induced corrosion or carbonation induced corrosion aggravated by chlorides. There was a variation in the condition of the reinforcement exposed within the undercroft wherein some locations, the steel was found to be clean and uncorroded while in other locations, complete loss of section was observed. Conventional concrete patch repairs and cathodic protection were undertaken on the elements forming the undercroft as well in other parts of the building, totalling more than 1000 patch repairs (Pierce., 2013).

3. 0 FIELD INVESTIGATION

Figure 2 presents several pictures of damaged concrete in the undercroft of BH4. Based on the visual observations shown in Fig. 2, the concrete damage process could be described as follows:

- General view looking across the undercroft. Note the faint green staining to the elements indicating the typical level of the tides (shown in Fig. 2(a))
- Green vegetation growth possibly indicating historic water penetration into the structure (shown in Fig. 2(b)).
- Exploratory breaking out into an area of spalling. Note the condition of the reinforcement with some loss (shown in Fig. 2(c))
- Sub-efflorescence, rusts staining and repair (shown in Fig. 2(d))

Fig. 2. Deteriorated concrete in the undercroft (Coats *et al*., 2015)

Concrete debris was collected from the undercroft of BH4. Pieces of around 10-20 mm in size were embedded in resin, polished and coated to be examined by using a Zeiss EVO MA10 Scanning Electronic Microscopy (SEM) and Energy Dispersive Spectrometer (EDS) for analysis. Images were extracted from each sample. Figure 3 and Table 1 illustrate some of these samples.

Fig. 3. SEM sample coated with carbon

Table 1. Description of the concrete debris

Sample	Location-Description	Test Methods
No. 1	Main building-extracted from skip-original concrete with some corroded steel	SEM
No. 2	Historic repair sample extracted from the slipway of the undercroft	SEM
No. 3	New repair material retrieved from the undercroft	SEM
No. 4	Original concrete retrieved from the undercroft	SEM
No. 5	Concrete sample from the slipway sandbags	SEM

3.1 Laser Scanning

Three small patches of concrete located in the undercroft were chosen to be monitored using a NextEngine 3D laser scanner to document material changes due to the exposure to weathering/seawater. These patches are presented in Figs. 4, 5 and 6.

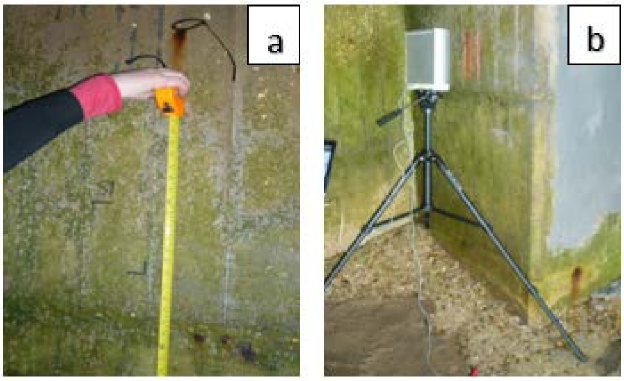

Fig. 4. Patch 1: (a) Shows the dimensions, (b) Shows the scanner set up

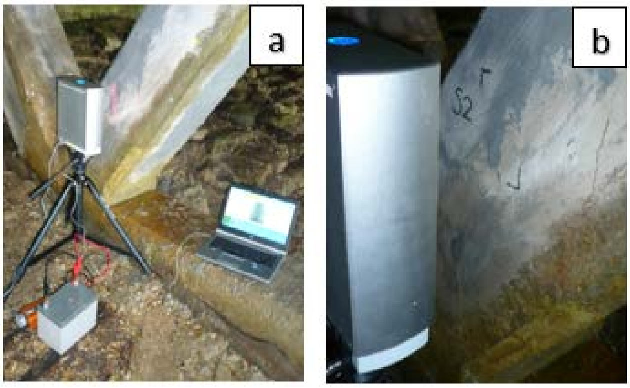

Fig. 5. Patch 2 truss element: (a) shows the scanner, external battery and laptop for data acquisition, (b) Shows an up-close view of the scanned area

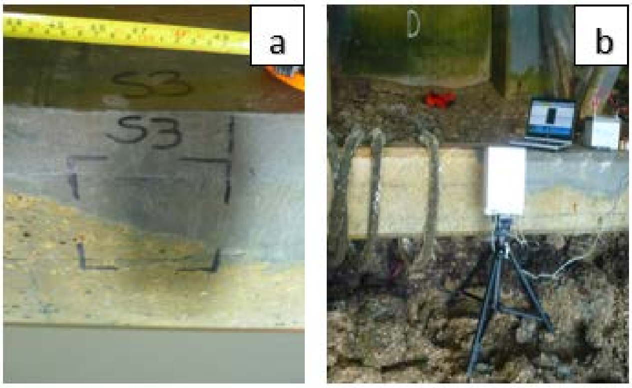

Fig. 6. Patch 3: (a) shows the dimensions, (b) Shows the scanner set up

Patch 1 identifies the presence of algae growth on concrete. The patch is located on a wall, slightly above the high tide level. The scanned area is 160 mm h x 100 mm w (shown in Fig. 4 (a) (b)).

Patch 2 is located on a diagonal truss element, slightly below the high tide level. The scanned area is 130 mm h x 90 mm w (shown in Fig. 5 (a) (b)). The white area on the top left-hand side of the scan identifies brushstrokes where a patch repair has been applied to the truss, so the patch includes both original concrete and repair materials.

Patch 3 is located on a horizontal beam, closer to the low tide level than the other sites. The scanned area is 135 mm h x 95 mm w (shown in Fig. 6 (a) (b)). Each patch was scanned three times over the space of three years. Data from two sets of scans taken 9 months apart are presented here.

4.0 RESULTS AND DISCUSSION

4.1 Microscopic Analysis

Figure 7 shows Backscattered electron image (BSE) of concrete with some rust from corroded steel which has gradually been washed out of the concrete (white areas on the image). Mapping of elements of this region given in Fig. 8 shows the presence of S (sulphur), Na (sodium) and Cl (chlorine) which is an indication of the presence of sodium sulphate ($Na_2 SO_4$) and sodium chloride (Na Cl).

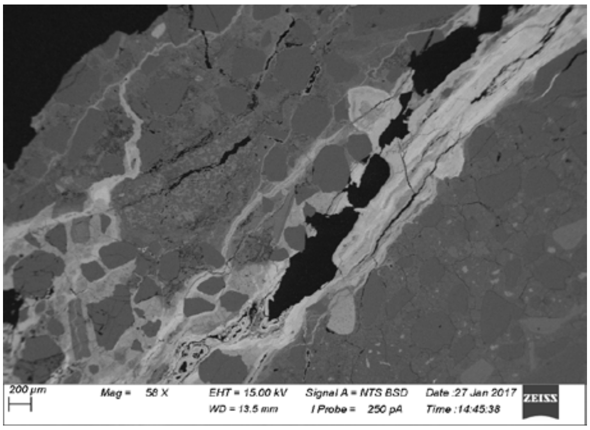

Fig. 7. Backscattered electron image (BSE)

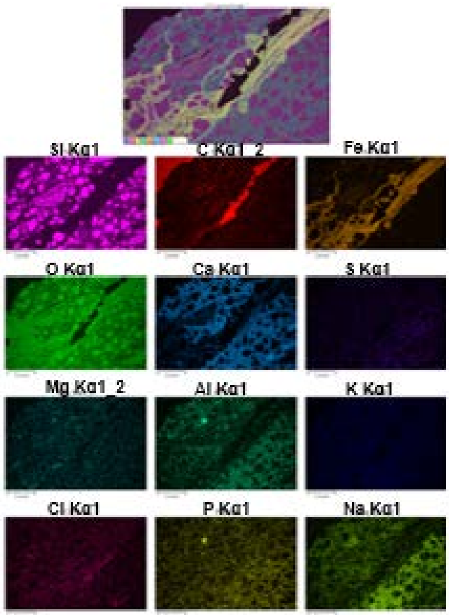

Fig. 8. Element mapping of Fig. 7

Figure 9 shows Backscattered electron image (BSE) of concrete with a cluster of particles similar in appearance to belite nest (Pintér & Gosselin, 2015) However, element maps show no Ca in the darker particles which are rich in Si only. Fig. 10 illustrates the mapping of elements in this region.

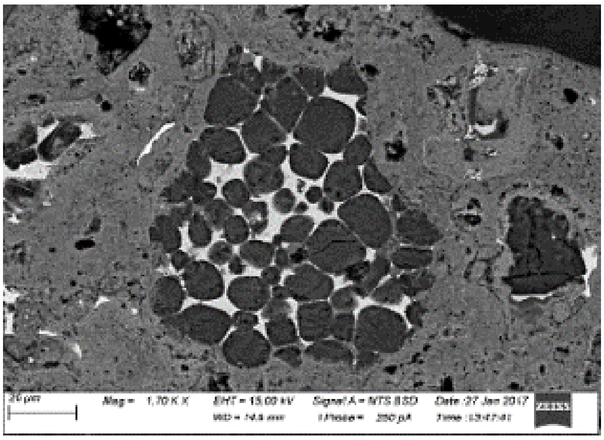

Fig. 9. Backscattered electron image (BSE)

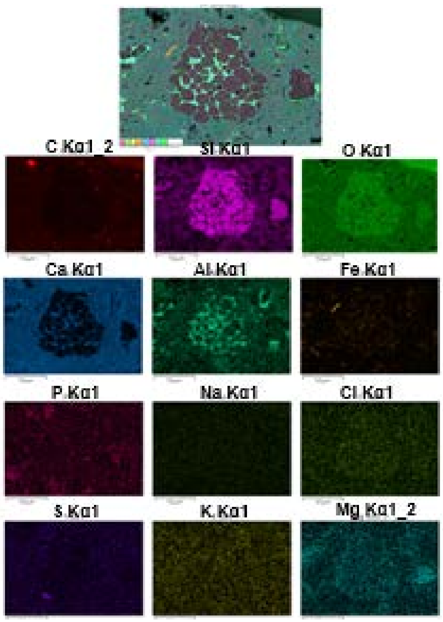

Fig. 10. Element mapping of Fig. 9

4.2 Laser Scanning

Figures 11, 13 and 15 illustrate the laser scanning results from the concrete patches which were chosen for monitoring. These patches were scanned to obtain high-resolution 3D images of the concrete surface so that gradual changes to the appearance and texture of the concrete surface and associated repairs could be detected. For the post-processing of the data, CloudCompare (CC) (is an open source 3D point cloud and mesh processing software designed to perform a comparison between two dense 3D point clouds) (Lague *et al*., 2013), and Surfer (to generate two and three-dimensional surface contour plots) were used for the analysis.

An estimation of the local surface roughness of the clouds was measured based on Gaussian statistics by using CloudCompare. The standard deviation of each cloud was obtained and used as a measure of local roughness.

Figure 11 illustrates the surface topography of patch 1: (a) reference (first) scan, (b) compared (second) scan 9 months later. The global values are very similar. However, there are some localized feature changes.

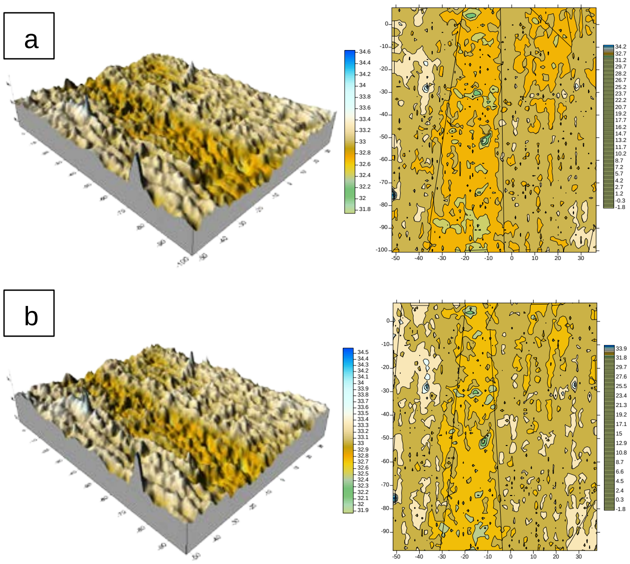

Fig. 11. Generated 3D and contour maps of patch 1 using Surfer software: (a) Reference scan (first scan), (b) Compared (second scan) 9 months later

Standard deviation is a key to measuring surface variation and a good indicator of surface roughness. Based on Gaussian statistics, local standard deviation STD cloud 1 and 2 of patch 1 was measured and it indicates the local roughness of each cloud.

Figure 12 illustrates a histogram plot of (a) cloud 1 (reference), (b) cloud 2 (compared). The statics illustrate no significant changes as the roughness has not considerably changed with standard deviations being 0.014 mm and 0.017 mm for the firs and second scans.

Figure 13. illustrates the surface topography of patch 2, (a) reference (first) scan, (b) compared (second) scan 9 months later. The maps clearly show almost every points are the same in relation to every other point. No changes could be detected.

The results below indicate the surface roughness is consistent over time where the standard deviation is 0.023 mm in both scans as shown in Fig. 14 (a) (b).

Figure 15 illustrates the surface topography of patch 3, (a) reference (first) scan, (b) compared (second) scan 9 months later. Changes in surface form have occurred at some particular locations. This patch is

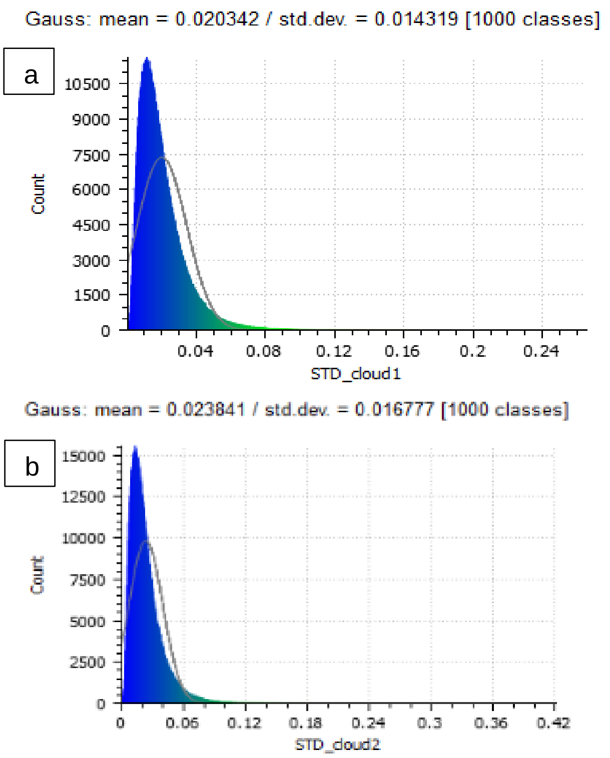

Fig. 12. Histogram plot of STD cloud 1&2

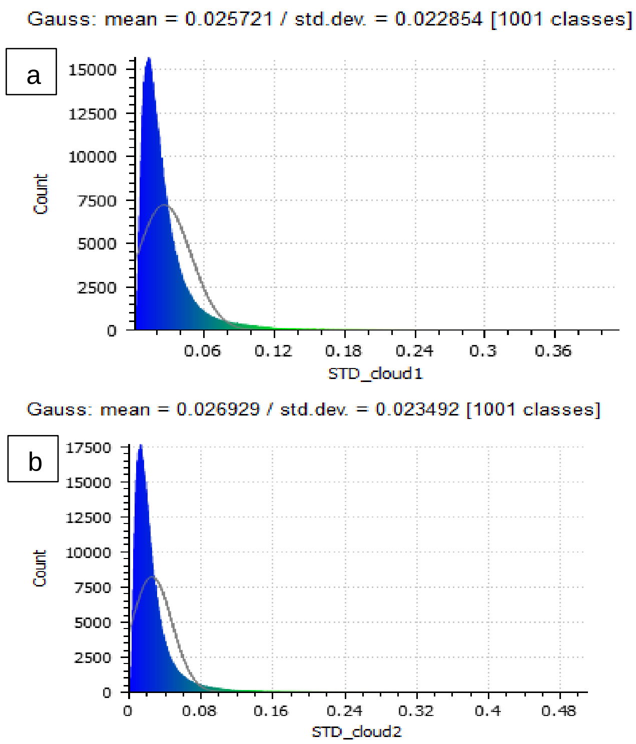

Fig. 14. Histogram plot of STD cloud 1&2

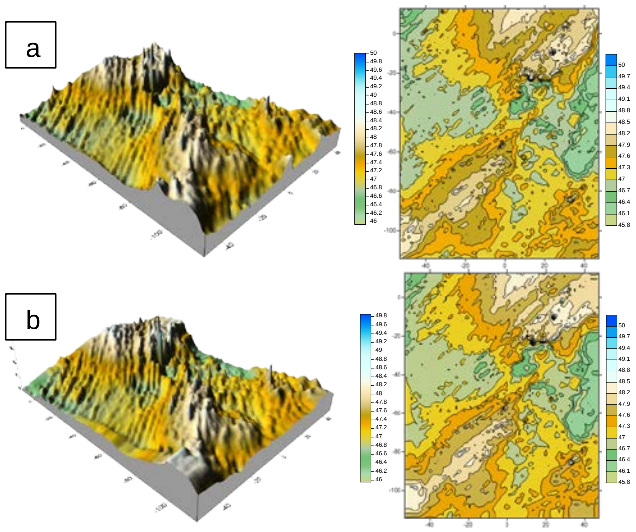

Fig. 13. Generated 3D and contour maps using Surfer software: (a) Reference scan (first scan), (b) Compared (second scan) 9 months later

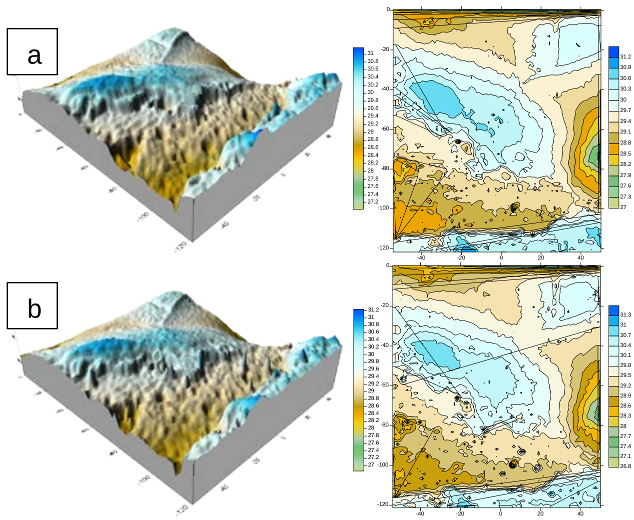

Fig. 15. Generated 3D and contour maps using Surfer software. (a) Reference scan (first scan). (b) Compared (second scan) 9 months later.

closer to the seawater, so changes in the surface are expected to occur more rapidly than other patches. It reflects the exposure of the surface concerned. Moreover, visual evidence identifies a change in colouring to the repair material over time (as shown in Fig. 16).

The roughness has increased over time between the two clouds where the standard deviation in cloud 1 is 0.022 mm compared to cloud 2 which is measured at 0.038 mm (as shown in Fig. 17 (a) (b)).

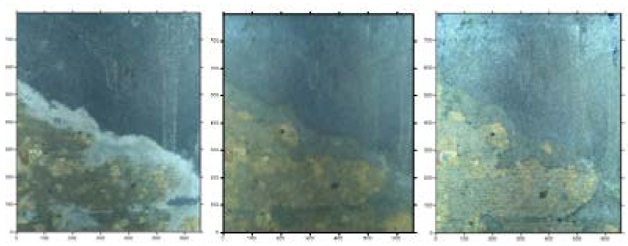

Fig. 16. Repair colour changes over time

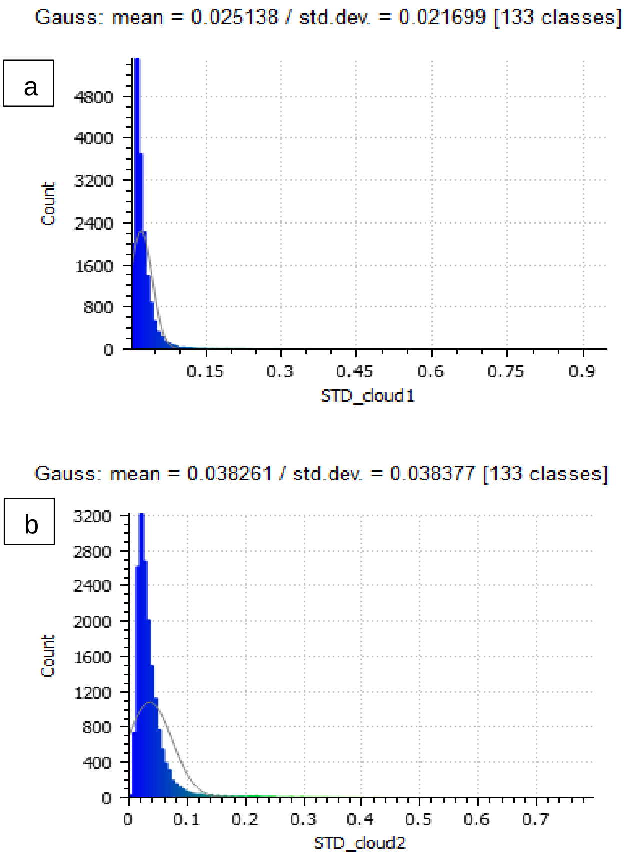

Fig. 17. Histogram plot of STD cloud 1&2

5.0 CONCLUSIONS

A field investigation on monitoring historic concrete and associated cementitious repair were conducted. 3D points cloud data derived from the NextEngine 3D laser scanner were analysed using CC. Results show topographic changes are detectable using laser scanning in combination with powerful software such as CloudCompare and Surfer. The NextEngine 3D scanner has proved to be capable of providing high precision data. However, it is only used for small objects or small areas of a surface. From a conservation perspective, this adopted methodology can be applied to any concrete structure to increase our understanding of rates of change to surface appearance and texture, which must be considered in greater depth in order to protect future heritage concrete structures.

The main limitation of the technique adopted here is that only a relative measurement can be made in the form of a standard deviation measurement to quantify surface texture. Further work has been carried out as part of this project using the scanner on laboratory specimens where fixed control points will enable absolute measurements of change to be made.

Acknowledgement

The authors express their gratitude to Peter Lambert, Portsmouth Naval Base Property Trust and the International Boatbuilding Training College. Also we would like to thank Total Access for providing safe access to the study site, as well as Gary Etienne and Elyas Zanjani from the School of Civil Engineering and Surveying, University of Portsmouth for their assistance.

References

Coats, A., Davies, J. D., Evans, D., & Riley, R., 2015. 20th century naval dockyards : Devonport and Portsmouth characterisation report. part 3. Naval Dockyards Society. Retrieved from https://researchportal.port.ac.uk/portal/en/publications/20th-century-naval-dockyards(aa8079d1-598c-43f5-8d63-07b48b0ff1c0).html

Lague, D., Brodu, N., & Leroux, J., 2013. Accurate 3D comparison of complex topography with terrestrial laser scanner: Application to the Rangitikei canyon (N-Z). ISPRS Journal of Photogrammetry and Remote Sensing, 82, 10–26. https://doi.org/10.1016/j.isprsjprs.2013.04.009

Meroño, J. E., Perea, A. J., Aguilera, M. J., & Laguna, A. M., 2014. Recognition of materials and damage on historical buildings using digital image classification. *South African Journal of Science*, *111*(12). Retrieved from http://www.sajs.co.za

Moses, C., Robinson, D., & Barlow, J., 2014. Methods for measuring rock surface weathering and erosion: A critical review. Earth-Science Reviews, 135, 141–161. https://doi.org/10.1016/j.earscirev.2014.04.006

Mukupa, W., Roberts, G. W., Hancock, C. M., & Al-Manasir, K., 2016. A non-destructive technique for health assessment of fire-damaged concrete elements using terrestrial laser scanning. Journal of Civil Structural Health Monitoring, 6(4), 665–679. https://doi.org/10.1007/s13349-016-0188-1

Pagounis, V., Tsakiri, M., Zacharis, V., Andritsanos, V., & Tsiardaki, M., 2016. Detection of geometric changes for an historic theatre by comparing surveying data of different chronological periods. Journal of Cultural Heritage, 21, 860–868. https://doi.org/10.1016/j.culher.2016.02.004

Pierce, N., 2013. Condition Assessment of Boathouse 4, Portsmouth Dockyard, HM Naval Base, Portsmouth (Vol. 490).

Pintér, F., & Gosselin, C., 2015. Material characteristics of prefabricated concrete elements from a late 19th century church in lower Austria Material characteristics of prefabricated concrete elements from a late 19 th century church in lower Austria, (June).

Schaefer, M., & Inkpen, R., 2010. Towards a protocol for laser scanning of rock surfaces. Earth Surface Processes and Landforms, 35(4), 417–423. https://doi.org/10.1002/esp.1938